

# Recent ice ages on Mars

James W. Head<sup>1</sup>, John F. Mustard<sup>1</sup>, Mikhail A. Kreslavsky<sup>1,2</sup>, Ralph E. Milliken<sup>1</sup> & David R. Marchant<sup>3</sup>

<sup>1</sup>Department of Geological Sciences, Brown University, Providence, Rhode Island 02912, USA

<sup>2</sup>Astronomical Institute, Kharkov National University, Kharkov, 61077, Ukraine

<sup>3</sup>Department of Earth Sciences, Boston University, Boston, Massachusetts 02215, USA

**A key pacemaker of ice ages on the Earth is climatic forcing due to variations in planetary orbital parameters. Recent Mars exploration has revealed dusty, water-ice-rich mantling deposits that are layered, metres thick and latitude dependent, occurring in both hemispheres from mid-latitudes to the poles. Here we show evidence that these deposits formed during a geologically recent ice age that occurred from about 2.1 to 0.4 Myr ago. The deposits were emplaced symmetrically down to latitudes of  $\sim 30^\circ$ —equivalent to Saudi Arabia and the southern United States on the Earth—in response to the changing stability of water ice and dust during variations in obliquity (the angle between Mars' pole of rotation and the ecliptic plane) reaching  $30\text{--}35^\circ$ . Mars is at present in an 'interglacial' period, and the ice-rich deposits are undergoing reworking, degradation and retreat in response to the current instability of near-surface ice. Unlike the Earth, martian ice ages are characterized by warmer polar climates and enhanced equatorward transport of atmospheric water and dust to produce widespread smooth deposits down to mid-latitudes.**

Of the planets in the Solar System, the climate of Mars is most similar to that of the Earth. Small quasi-periodic variations in the Earth's orbit and spin parameters over timescales of  $10^4\text{--}10^5$  years drive large-scale changes in climate<sup>1,2</sup>. Similarly, Mars exhibits variability of its orbital and axial elements with timescales comparable to the Earth's; however, the ranges of Mars' variations are significantly greater. Over the past 10 Myr, Earth's obliquity has ranged from  $22^\circ$  to  $24.5^\circ$ , while for Mars<sup>3–6</sup> the range was  $14^\circ$  to  $48^\circ$ . Similarly, the eccentricity of Earth's orbit varied from 0 to 0.06, while for Mars the range was 0 to 0.12. The consequent changes to insolation and seasonality at middle to high latitudes on Mars have inevitably caused significant changes in the seasonal cycles of carbon dioxide, water and dust<sup>7,8</sup>. Thus Mars may have experienced the most significant quasi-periodic variations in its climate over the past 10 Myr of any planet in the Solar System.

Analysis of data from spacecraft missions before Mars Global Surveyor (MGS) identified laminations and layers in the north and south polar caps whose origin was attributed to quasi-periodic climate change<sup>9</sup>. Theoretical modelling of water vapour diffusion in near surface soils predicted that ground-ice stability in the mid-latitudes would vary in concert with the orbital and axial forcing<sup>10</sup>. An array of landforms in the mid-latitudes of Mars were catalogued<sup>11</sup> that have analogues to ice-rich terrains on Earth. However, their ages appeared to be significantly greater than 10 Myr, and their origin was not linked to quasi-periodic climate change. Here we use data from the recent Mars missions (MGS and Odyssey) to show multiple lines of evidence for surface deposits that formed as a result of recent quasi-periodic climate change on Mars. The observations span a large range of scales (metres to kilometres to hundreds of kilometres), are of diverse nature (morphology, topography and chemistry), and are remarkably consistent with models of current and past ground-ice stability. These results all point to the presence of a succession of metres-thick, latitude-dependent surface deposits that are young, ice-rich when formed, and whose deposition and removal is driven by climate change that is induced by spin-axis tilting.

## MGS observations

The subkilometre-scale roughness derived from global Mars Orbiter Laser Altimeter (MOLA) data revealed smoothing at subkilometre scales above about  $30^\circ$  latitude in both hemispheres<sup>12</sup> (Fig. 1a). This topographic smoothing was attributed at least partly to a surface deposit several metres thick that was superposed, or draped on, older geological units (Fig. 2) and referred to as a mantle<sup>12–14</sup>. The

statistics of the kilometre- and subkilometre-scale topography of Mars are influenced by such a metres-thick mantle because the typical topographic slopes at these scales are of the order of a degree or less; this means that the typical vertical scale of topography is two orders of magnitude shorter than the spatial scale. Another prominent latitudinal trend is seen in topographic concavity at hundreds of metres baseline (Figs 1b and 3c), a measure of the relative balance of concave and convex segments of topographic profiles<sup>13</sup>.

Analysis of Mars Orbiter Camera (MOC) images revealed the distribution of many geological features that also exhibit a latitude dependence<sup>15–23</sup>. A systematic study of the presence or absence of a specific morphology representing a metres-thick but partially degraded and discontinuous surface deposit (Fig. 2c–f) showed that this terrain was limited to the  $30^\circ\text{--}60^\circ$  north and south latitude zone (Figs 1c and 3b)<sup>16</sup>. This deposit was interpreted as a recent, formerly ice-rich dust mantle that originated as a thin blanketing airfall layer and was now undergoing dissection and removal<sup>16</sup>. There was no evidence of this deposit in equatorial and low-latitude regions (between  $30^\circ$  N and  $30^\circ$  S)<sup>16</sup>. Poleward of  $60^\circ$ , this mantle was continuous and commonly characterized by a unique bumpy texture at the scale of several tens of metres that often resembled the surface of a basketball (Fig. 2a), and lineated and wrinkled versions of this terrain type<sup>12–16,22,23</sup>. Evidence for multiple layers (Fig. 2b) within the mantle unit has been documented, indicating several generations of deposition and removal<sup>13,20</sup>.

Different types of polygons and patterned ground were also noted to occur preferentially above  $30^\circ$  north and south latitude<sup>17,18</sup>, suggesting the presence of a dynamic layer in which near-surface ice-rich material was undergoing thermal cycling. Startling images show what appear to be very recent water-carved gullies that occur preferentially in this region and have been interpreted to represent groundwater sapping<sup>19</sup>, melting of ground ice<sup>24</sup> or snowpack during higher obliquity<sup>25</sup>, or local microclimate conditions<sup>26</sup>. Viscous flow features<sup>20</sup> and related deposits<sup>21</sup> suggestive of mobilization and flow of ice-rich mantling materials occur in the same latitude band. Results from the  $\gamma$ -ray and neutron spectrometers on board Mars Odyssey<sup>27–29</sup> showed the distribution of hydrogen within the top metre of the martian surface. The high concentrations of hydrogen at polar latitudes were interpreted to indicate the presence of water ice (at  $>50\%$  by mass) in the near subsurface, below a hydrogen-free surface sediment layer tens of centimetres thick<sup>30</sup>. The global distribution of hydrogen and interpreted water abundance<sup>30</sup> on Mars (Fig. 1e) shows a remarkable correlation with the latitude-dependent deposits interpreted from the MOLA and MOC data<sup>31</sup>.

Furthermore, it shows a very high correlation with the present stability of near-surface ground ice (Fig. 1d) as modelled from the diffusive exchange of water vapour between the regolith pore space and the martian atmosphere<sup>10,32</sup>.

Latitude is the single variable with which all of these diverse observations correlate, and climate is the only process known to be latitude-dependent. Degradation of the youthful mantle in the mid-latitudes suggests a very recent change in climate<sup>16</sup>. The remarkable correspondence (Fig. 1) between the character of the terrain smoothness, the continuity of the mantle, the high hydrogen

abundance, and the theoretical stability of ice in the near-surface soil provide compelling evidence for climate-driven water ice and dust mobility, emplacement and dissection. What do the characteristics of these regions and deposits tell us about the nature and timing of such activity?

**Interpretations of deposits**

One explanation for the correlation between the observations and models is that we are simply observing an outcome of climate-related diffusive exchange of water vapour between the regolith pore

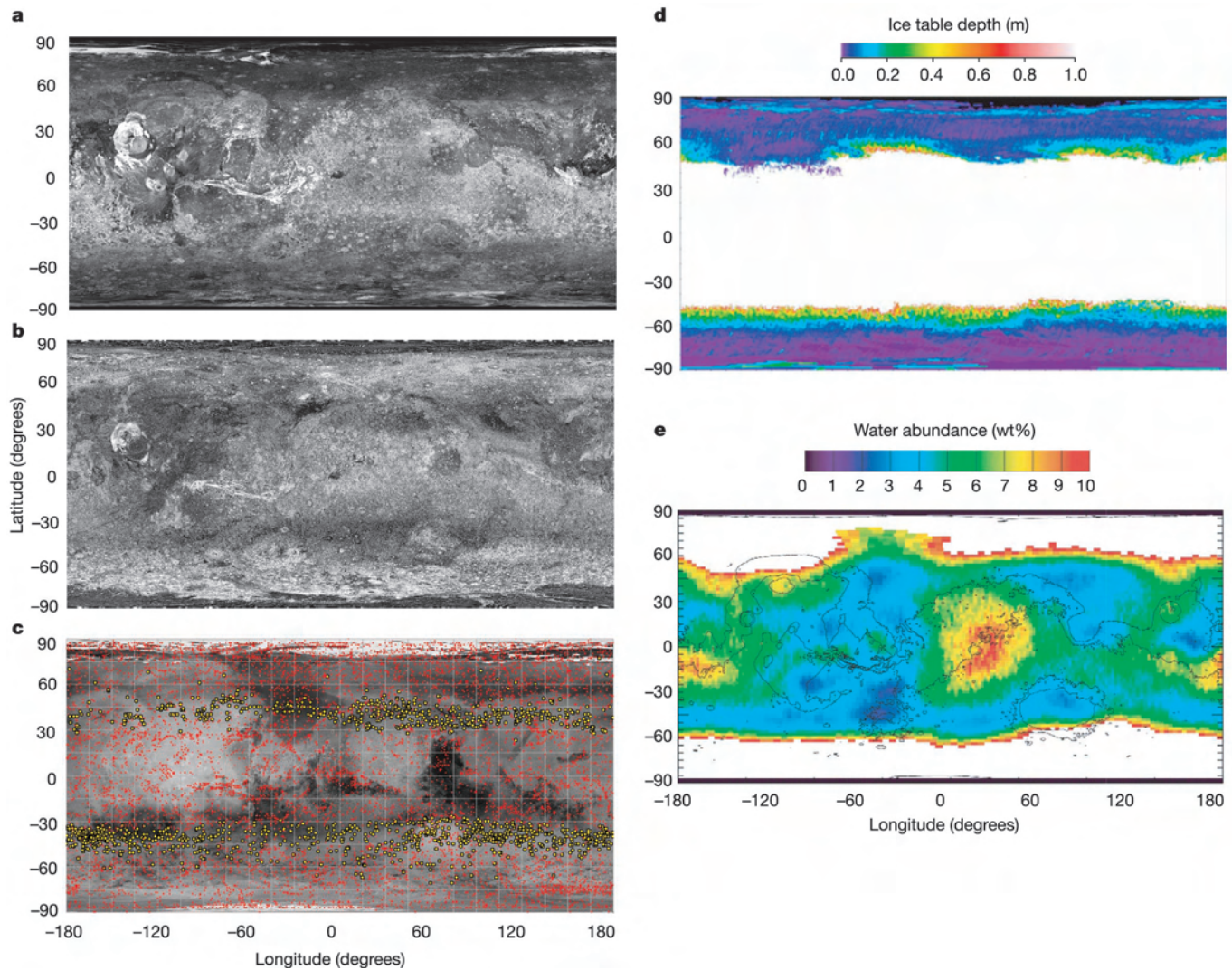


**Figure 1** Maps showing important latitudinal trends on Mars (simple cylindrical projection). **a**, Subkilometre-scale topographic roughness. Brighter shades denote a rougher surface. The roughness parameter mapped is the interquartile width of the frequency distribution of the differential slope<sup>12</sup> at 0.6 km baseline. **b**, Subkilometre-scale topographic concavity. Brighter shades denote higher prevalence of concave topography. The parameter mapped is the median curvature of topographic profiles at 0.6 km baseline normalized by the interquartile width of the curvature–frequency distribution<sup>13</sup>. Most of the geologic units in the equatorial zone have some concave topography (positive concavity). The high-latitude zones have higher positive concavity (Fig. 3c). Smooth filling of local lows by the mantle here eliminates smaller-scale topographic variations and in this way amplifies the concavity. The mid-latitude zones (30°–60°) exhibit a distinctive low concavity that differs from both unmantled equatorial and high-latitude mantled regions<sup>13</sup>. This is interpreted to be related to dissection of the mantle<sup>13–16</sup>, small-scale irregular topographic variations due to dissected and patchy mantle occurrence in these zones cause randomly alternating concave and convex profile segments and concavity values close to zero. All data in **a** and **b** are derived from statistics of all along-track

topographic profiles obtained by MOLA. **c**, Distribution of examined MOC images. Yellow circles indicate MOC images with dissected mantle terrain, red circles indicate images with no apparent dissected terrain<sup>16,20</sup>. The mantle is interpreted to be present poleward of ~60°, but is not dissected. An albedo mosaic is used as a background. **d**, Map of ice table depth for an annual mean of 10 precipitable micrometres of atmospheric water vapour based on a near-surface ice stability model<sup>32</sup>. In this model, ice in the near subsurface is unstable at low latitudes (equatorial regions, no ice-rich mantle terrains observed) and stable at high latitudes (polar regions; thick, intact ice-rich mantles observed). The mid-latitude regions are transitional zones in which ice is currently unstable, corresponding to areas where we observe degraded, previously ice-rich deposits such as the dissected mantle terrain. This model of ice stability shows a remarkable correlation with the observations of ice-rich deposits from Odyssey<sup>27–30</sup> and MGS data. **e**, Mars Odyssey GRS/NS experiment data showing interpreted water abundance in weight per cent<sup>30</sup>. White areas above ~60° latitude are interpreted as ice buried a few centimetres below the surface<sup>30</sup>.

space and the martian atmosphere. The depth to ice below the surface is predicted to have varied vertically in the regolith and with latitude as Mars experienced various orbital cycles in its most recent history<sup>10</sup>. In this scenario, the latitude-dependent surface textures in the 30°–60° zones would be due to reworking of the surface caused by repeated diffusive precipitation and subsequent sublimation of water ice during recent excursions in ground-ice stability. The 30°–60° zones would thus represent a zone of dynamic exchange between regolith and polar water reservoirs, while regions poleward of 60° represent a remnant stable deposit of water ice in the regolith under current conditions. In this scenario<sup>10,32</sup>, no significant amounts of new material would be deposited on the surface.

There is, however, abundant evidence for deposition of dust–ice mixtures and layering (Fig. 2). Superposition relations are common<sup>16</sup>, dissection in the 30°–50° latitude range shows removal and exposure of underlying units<sup>16</sup>, and multiple layers are seen,

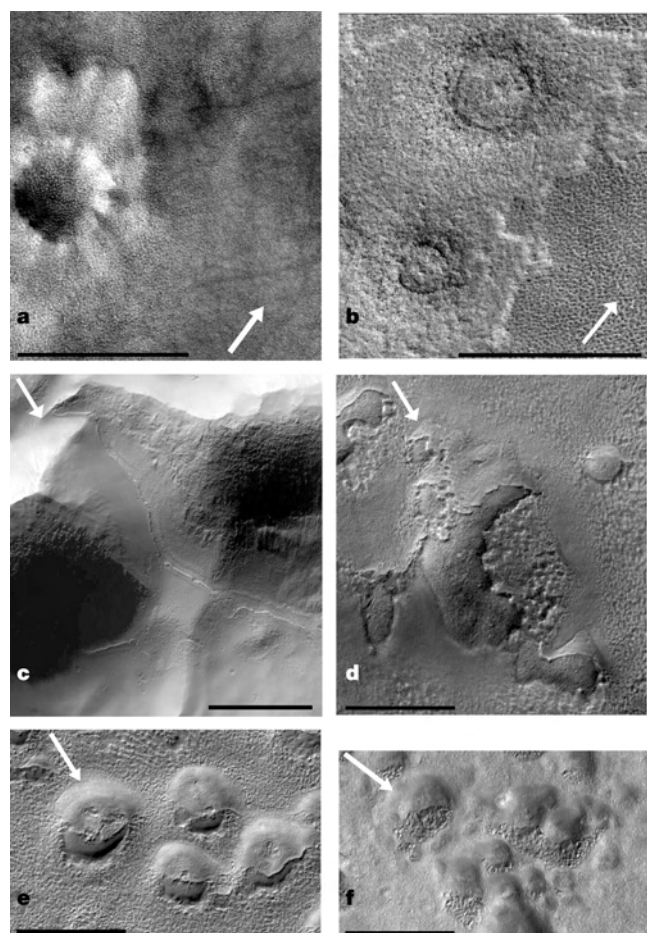


**Figure 2** Characteristic tens of metre-scale textures of the mantle and dissected terrain as seen in MOC high-resolution images<sup>15,16</sup>. Scale bars at the bottom of each image are 1 km; north is at the top. Arrows show the illumination direction. **a**, Homogeneous mantle with basketball texture covers well-preserved crater and its ejecta. Portion of MOC image E02-01380; 61° N, 210° W. **b**, A mantle layer with the basketball texture partly removed. Co-registered MOLA profile shows a 3–4 m height for the topographic step across the mantle layer boundary. Two circular features are probably old, heavily degraded, mantled impact craters. Portion of MOC image M02-01316; 69° N, 150° W. **c**, Example of dissected mantle terrain with internal layering found in the mid-latitudes. The mantle is smooth and has been removed from the pole-facing slopes. The removal of the mantle on the shaded side of the rightmost knob has revealed an underlying mantle layer. Portion of MOC image M20-00144; 35° S, 174° W. **d–f**, Examples of dissected mantle found in the mid-latitude regions where the mantle has been preferentially removed from pole-facing slopes. **d**, Portion of MOC image M04-02856; 47° S, 218° W. **e**, Portion of MOC image FHA-01450; 44° S, 240° W. **f**, Portion of MOC image M04-02289; 43° S, 240° W.

particularly toward the poles<sup>13</sup>. The latitudinal trend of subkilometre-scale roughness is readily explained by the deposition of a metres-thick smooth layer on top of underlying terrain<sup>12</sup>. Such a deposit explains the observed increase of topographic concavity above 60° latitude<sup>13</sup>, while the decrease in concavity in the 30°–60° zones is interpreted to be related to dissection of the mantle<sup>13,16</sup>. The extreme morphological homogeneity of the unit above 60° latitude and the manner in which it drapes subjacent deposits<sup>22</sup> also supports deposition of a mantle. The very low abundance of superposed impact craters<sup>13,16,23</sup> supports a very youthful age (<10 Myr), and the paucity of subkilometre-scale degraded impact craters<sup>23</sup> supports deposition, mantling and obscuration, rather than *in situ* reworking. The very high near-surface water-ice content inferred from the Odyssey  $\gamma$ -ray and neutron spectrometer data<sup>27–30</sup> is consistent with a model of deposition of a relatively uniform ice-rich dust layer from the atmosphere. Other evidence for the ice-rich nature of the deposit includes the correspondence of its continuous extent with modelled ground-ice stability<sup>10,32</sup>, its apparent mechanical strength<sup>20</sup>, evidence for creep on steep slopes<sup>20,39</sup>, and its relation to water and ice-related features (such as viscous flow, and polygons)<sup>19–21,24,25</sup>. The weight of the geological observations points to airfall deposition.

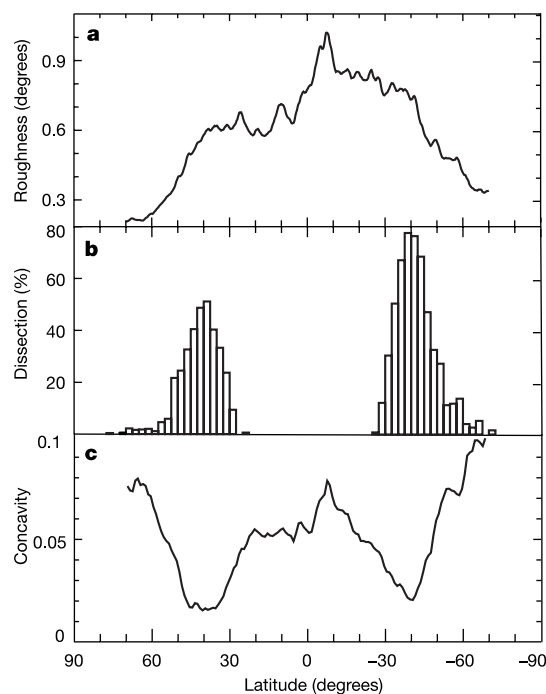


**Figure 3** Latitudinal dependence of statistical characteristics of subkilometre-scale surface topography (roughness and concavity) and percentage of images with dissected terrain. Southern latitudes are shown as negative values. **a**, Roughness parameter plotted is the interquartile width of the frequency distribution of the differential slope<sup>12</sup> at 0.6 km baseline. The peak at 10° S is related to the Valles Marineris complex; the difference in roughness between 20–40° S and 20–40° N reflects the geological dichotomy of Mars, with prevalence of rough heavily cratered highlands in the southern hemisphere and smoother lowlands in the northern hemisphere. The decrease of roughness poleward from 40° N and 40° S does not correlate with large geomorphological features and reflects the latitudinal smoothing trend. **b**, Percentage of high-resolution MOC images having the characteristic dissected morphology among 15,000 images surveyed<sup>16</sup>, in 2.5° latitude bins. There are two peaks in the presence of the dissected mantle at 41° N and 41° S, which correspond to the latitude in **a** where smoothing begins. **c**, Topographic concavity. The parameter plotted is the median curvature of topographic profiles at 0.6 km baseline normalized by the interquartile width of the curvature–frequency distribution<sup>13</sup>. A strong decrease of concavity is observed within the 30–50° zone in both hemispheres and correlates well with the occurrence of dissected terrains.

Integration of observations and climate models

We propose a model that explains the observations by the deposition and removal of mixtures of dust and water ice, and is controlled by climate variations resulting from quasi-periodic variations in orbital parameters. During periods of high obliquity ( $>30^\circ$ ), increased summer insolation on the polar regions results in greater water vapour release from the polar caps, increasing the atmospheric water vapour content and thus the humidity<sup>33,34</sup>. Higher humidity moves the latitude of subsurface ice stability closer to the equator, and within the soil profile, closer to the surface<sup>10</sup>. Climate models predict that ice removed from the poles is deposited on the surface at these lower latitudes where it persists throughout the year<sup>35–38</sup>. Mars global circulation model (GCM) simulations also predict strong winds favourable for dust lifting from global reservoirs and redistribution during such times<sup>35,36</sup>. This dust is readily incorporated into the growing ice deposits. These three factors (increased atmospheric water vapour content, increased atmospheric dust content, and shifting of the surface ice stability zone toward the equator) are thus predicted to act in concert at high obliquity to produce the latitude-dependent deposits that we observe. Owing to the higher year-average and summer-average polar temperatures and denser atmosphere, the transport of water at high obliquities is predicted to be rapid<sup>37</sup>. High obliquity periods favourable to this process are of the order of 40 kyr (Fig. 4)<sup>5</sup>, long enough to provide deposition of at least several metres of ice-rich material<sup>37</sup>. Thus, in our model the deposited layers should be geologically recent, latitude-dependent, dust–ice mixtures, superposed on underlying terrain, and varying in their character as a function of latitude.

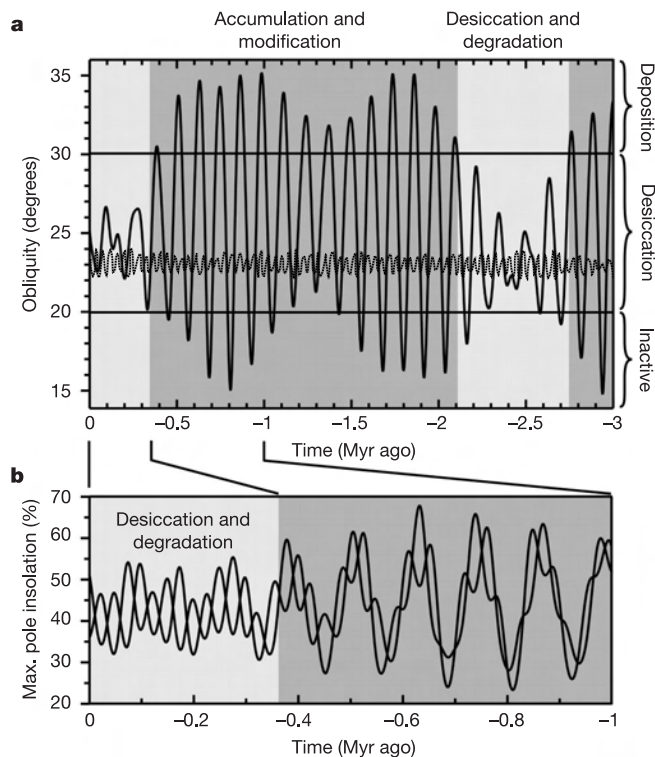


**Figure 4** Orbital forcing of climate in the past. **a**, Obliquity variations<sup>5</sup> for the past 3 Myr, with glacial (accumulation and modification; dark grey) and interglacial (desiccation and degradation; pale grey) periods marked. Low-amplitude line between  $22^\circ$  and  $24^\circ$  represents the obliquity range on Earth during the comparable period of history<sup>5</sup>. **b**, Maximal insolation of the north and south poles<sup>5</sup> for the past 1 Myr. During the past 300 kyr, there is an asymmetry in insolation, but before 300 kyr ago, insolation is primarily driven by obliquity and is symmetric.

As obliquity decreases, the surface ice stability zones shrink toward the polar caps and ice sublimates from the uppermost layer of the mantle, creating a protective ice-poor crust analogous to the sublimation of ice from loess on Earth<sup>39</sup>. At lower obliquity, water remains sequestered in cold polar regions and the atmospheric humidity is decreased. Under this drier atmosphere, calculations suggest poleward shrinking of this ice-rich mantle and widespread desiccation<sup>10</sup> between  $30^\circ$  and  $60^\circ$ . As the ice sublimates, it leaves behind a weakly cemented, porous surface lag (analogous to the lags observed in the Fox permafrost tunnel<sup>39</sup>) that retards sublimation. If desiccation is severe and the remaining ice-poor regolith lacks a cohesive surface crust, then deposits will become susceptible to eolian disruption and destruction<sup>16</sup>. For high latitudes ( $>60^\circ$ ), ground ice is stable near the surface with obliquity as low as  $20^\circ$ , and thus over the past 10 Myr dissection would be most important in the mid-latitudes ( $30^\circ$ – $60^\circ$ ). The depth of desiccation is predicted to vary as the square root of time<sup>39</sup>, and thus the characteristic timescale of water loss increases with time and decreasing obliquity. Thus, low-obliquity periods are likely to be too short to desiccate and remove the mantle completely at all latitudes. Evidence for the present desiccation and removal of the mantle layers includes the dissected terrain in the  $30^\circ$ – $60^\circ$  north and south latitude zone<sup>16,20</sup> (Fig. 2e, f, and Fig. 3), the decrease of subkilometre-scale topographic concavity (Figs 1b and 3c) in this same latitude range<sup>13</sup>, and the correspondence of this zone with the latitudes predicted to be at present desiccated (Fig. 1e, f) in the near surface<sup>10,32</sup>.

A variety of surface features at higher latitudes ( $>60^\circ$ ) (for example, basketball-textured terrain and its variants, and polygons) are interpreted to represent the net effect of long-term orbital variations on relatively stable, debris-covered ice-rich deposits. In the Antarctic dry valleys, a cold-polar desert that represents a terrestrial analogue for regions with buried ice on Mars, such landforms are related to sublimation and thermal cycling of ice-rich sediments<sup>40,41</sup>. In Beacon Valley, sublimation of debris-rich ice produces a dry surface lag that insulates and slows loss of remaining ice<sup>41</sup>. Ground temperature cycling between  $<0^\circ\text{C}$  and  $\ll 0^\circ\text{C}$  creates tensile stresses that result in a network of hexagonal cracks, extending upward from buried ice to the ground surface (and vice versa). A lag of coarse-grained sublimation till forms on top of the ice, where fines sift into open thermal contraction cracks. Owing to these spatial variations in till texture, rates of sublimation vary across the ice surface. High rates occur below coarse-grained lags that cap contraction cracks, and low rates are found at polygon centres beneath fine-grained debris of low porosity and permeability. The high-centred ‘sublimation polygons of Beacon Valley may be analogous to the latitude-dependent polygonal basketball-textured terrain on Mars. If so, the ‘basketball’ terrain probably reflects a combination of long-term ice sublimation, coupled with thermal cycling on timescales both short (seasonal) and long (for example, obliquity)<sup>41</sup>. A close analogue for such modification on Earth includes long-term changes in the distribution and character of permafrost regions of the high Arctic<sup>42,43</sup> and Antarctic.

Estimates of the age of the mantling unit and its contained layers come from several sources. The number of small fresh craters is very low, and the crater retention age is correspondingly very young<sup>16</sup>, possibly as young as 150 kyr but most certainly less than 10 Myr. Stratigraphic relations show a complex history of successive episodes of deposition and removal<sup>13</sup>, suggesting that the mantle consists of multiple depositional cycles. Regional stratigraphic evidence at high latitudes<sup>9,14</sup> shows outliers of polar cap deposits as well as dark dunes locally superposed on the mantle. Finally, many of the surface textures of the mantle (for example, polygons, and basketball-textured terrain) are consistent with morphologies formed over several glacial cycles in the Arctic and Antarctic periglacial environments, suggesting that changing environmental conditions over extended time periods are required. Thus, taken together, the characteristics of the mantle suggest that the deposit is

geologically very young, but that it is composed of numerous sublayers and features requiring multiple depositional cycles.

Integrating the geologic evidence with the most recent orbital history of Mars results in a dynamic depositional–erosional model for ice in the mid–high latitudes (Fig. 4). The orbital and spin elements of obliquity, eccentricity, and the areocentric longitude of the Sun at perihelion ( $L_p$ ) (Fig. 4) all affect water-ice migration on Mars<sup>10,37</sup>, but with varying timescales and degree. Over the past 300 kyr the obliquity has remained relatively stable within a range of 22°–26° (Fig. 4). During this period, high eccentricity causes differences in seasonality of the northern and southern hemispheres (for example, the southern hemisphere today experiences shorter, warmer summers and longer winters than the northern hemisphere), while retarding of  $L_p$  causes the seasonality difference to reverse every ~25 kyr. If the retardation of  $L_p$  were the dominant driver of the deposition and erosion of the mantle, then we would expect the geologic evidence to be asymmetric in its preservation, reflecting the last such state (Fig. 4b). On a global scale, however, the geologic evidence is remarkably symmetric (Figs 1 and 3). But earlier than 300 kyr ago, obliquity regularly exceeded 30°, totalling 15 discrete excursions over the past 2 Myr, during which each excursion lasted of the order of 20–40 kyr. During this period, the high-amplitude obliquity oscillations dominate the insolation regime of the polar regions. When obliquity exceeds 30°, water ice is stable in the near surface down to the lower mid-latitudes<sup>10</sup>, and climate models predict that water ice is efficiently moved from polar cap reservoirs by sublimation and deposited in the mid-latitudes<sup>37</sup>. According to Mars climate models, each high-obliquity excursion would result in tens of metres of ice being removed from the poles; this material would then be transported, and deposited in the mid-latitudes with a water ice content equivalent to a few metres<sup>37</sup>, together with dust also eroded from the polar layered terrains<sup>9</sup>.

As the obliquity changes to values <30°, ice is sublimed from the mid-latitude deposits, creating a surface lag of dust analogous to that seen in Earth environments<sup>39,41</sup>. Such a lag deposit strongly retards further sublimation<sup>39</sup>. The lower year-average and summer temperatures at high latitudes at low obliquity decrease the diffusion rate of water vapour in the pores. Furthermore, as obliquity declines below 21°, the atmospheric pressure drops significantly with the sequestering of CO<sub>2</sub> in the polar caps<sup>44</sup>, further decreasing the diffusion rate in small pores and preventing eolian erosion of the lag. The effects of a retarding loess-like lag allows for all or part of the mantle deposited during a high-obliquity period to be preserved during the low-obliquity excursion. It is during the extended periods of moderate obliquity, such as for the past 300 kyr, that geologic processes have sufficient time to produce large-scale degradation of the mantle in mid-latitude zones.

Before 5 Myr ago, martian obliquity regularly exceeded 45° and the mean obliquity over this time was >35°, compared to a mean of 26° for the past 4 Myr (ref. 5). With obliquity >45° (>6 Myr ago), the polar sublimation rate is very high and ice is predicted to persist at the equator<sup>35</sup>. Given the relatively sharp boundary of the mantle at mid-latitudes and the lack of evidence of an extensive remnant mantle in equatorial regions<sup>16</sup>, we consider this time period a less likely option for formation of the present-day high-latitude mantle. If, however, mantle deposition and preservation is sustained by the mean obliquity, rather than the excursions, then the period before 5 Myr ago may be a more likely candidate.

### Ice ages on Mars

Integrating the observations with global climate models results in a martian ice age hypothesis (Fig. 4a). Between about 2,100 and 400 kyr ago, obliquity regularly exceeded 30° and water ice was removed from the polar reservoirs and transported to mid-latitudes, where it nucleated on dust particles in the air and/or at the surface and was deposited as a mantle. Though obliquity varied greatly during this time, the periods with lower obliquity were too short to allow for

complete erosion of the sublimation-retarding surface lags, preserving much of the mantle intact. We refer to such periods of net deposition (for example, between 2,100 and 400 kyr ago) as glacial periods. During the past ~300 kyr, obliquity has been near 25° with comparatively little variation. We refer to these times as interglacial periods (Fig. 4a). Water ice in the mid-latitudes has been slowly and steadily removed from this reservoir by diffusion, sublimation, and atmospheric transport processes; it was deposited in the polar regions, creating the uppermost layers in the polar cap<sup>45,46</sup>, and also resulting in the degradation of the surface mantle in the 30°–60° latitude bands. Because of the thinness of the deposit and the presence of admixed dust, the total volume of water is of the order of a metre global equivalent layer, and thus only a few per cent of the present volume of the polar caps. If the dissected portion of the deposit (30°–60° latitudes) contained ~50% by volume water ice, and half of this was removed by desiccation processes and deposited at the poles, it would form a layer several tens of metres thick on the polar caps.

We thus conclude that the emplacement of the ice- and dust-rich mantle extending from polar regions down to low mid-latitudes represents the equivalent of an ice age on Mars. If such an ice cover had occurred on Earth, it would have reached southward to latitudes equivalent to Saudi Arabia, North Africa and the southern United States. Poleward migration of the equatorward limit of the ice–dust-rich mantle, partial desiccation of the mantle in the latitudinal belt between 30° and 60°, and modification via sublimation and thermal cycling of long-lived ice-rich deposits poleward of 60°, represent some of the changes that occur during interglacial times (Fig. 4).

Martian ice ages as proposed here differ considerably from those on Earth<sup>7,47</sup>. First, terrestrial oceans are large heat reservoirs and distribution systems, and sinks for dust. Second, the major reservoir response during climate cycles on Earth is the amount of water stored in the polar caps; the major atmospheric gas components are not thought to change significantly. Third, orbital forcing factors thought to be the pacemaker for the timing of Earth's recent ice ages<sup>48</sup> are much less extreme than on Mars<sup>6</sup> (Fig. 4a) owing to the stabilizing presence of the Earth's Moon. On Earth, lower polar insolation causes the deposition of snow, and the formation and lateral spreading of continental ice sheets.

Mars, on the other hand, is characterized by a lack of oceans in its recent past, an abundant and mobile dust supply, and extreme orbital forcing factors. Its major atmospheric gas (CO<sub>2</sub>) is in dynamic equilibrium with its solid phase, resulting in the potential for significant changes in atmospheric CO<sub>2</sub> abundance and pressure<sup>49</sup>. Glacial periods on Earth are characterized by colder temperatures at the poles on average, while on Mars, the reverse is true.

In cold polar deserts on Earth, evidence has been cited for the preservation of glacial ice >8 Myr old at depths just below the surface<sup>50</sup>. Mars is characterized by an extremely cold polar desert environment, and we anticipate that the record of recent climate change on Mars is similarly preserved in the shallow subsurface over wide latitude expanses—and thus readily accessible to future robotic and human exploration. □

Received 16 May; accepted 8 October 2003; doi:10.1038/nature02114.

1. Imbrie, J. & Imbrie, K. P. *Ice Ages: Solving the Mystery* (Harvard Univ. Press, Cambridge, MA, 1986).
2. Zachos, J. *et al.* Trends, rhythms, and aberrations in global climate 65 Ma to present. *Science* **292**, 686–693 (2001).
3. Touma, J. & Wisdom, J. The chaotic obliquity of Mars. *Science* **259**, 1294–1297 (1993).
4. Laskar, J. & Robutel, P. The chaotic obliquity of the planets. *Nature* **362**, 608–612 (1993).
5. Laskar, J. *et al.* Orbital forcing of the martian polar layered deposits. *Nature* **419**, 375–377 (2002).
6. Ward, W. R. in *Mars* (eds Kieffer, H. H. *et al.*) 298–320 (Univ. Arizona Press, Tucson, AZ, 1992).
7. Kieffer, H. H. & Zent, A. P. in *Mars* (eds Kieffer, H. H. *et al.*) 1180–1218 (Univ. Arizona Press, Tucson, AZ, 1992).
8. Fanale, F. P. *et al.* in *Mars* (eds Kieffer, H. H. *et al.*) 1135–1179 (Univ. Arizona Press, Tucson, AZ, 1992).
9. Thomas, P. *et al.* in *Mars* (eds Kieffer, H. H. *et al.*) 767–795 (Univ. Arizona Press, Tucson, AZ, 1992).
10. Mellon, M. T. & Jakosky, B. M. The distribution and behavior of Martian ground ice during past and present epochs. *J. Geophys. Res.* **100**, 11781–11799 (1995).
11. Squyres, S. W. *et al.* in *Mars* (eds Kieffer, H. H. *et al.*) 523–554 (Univ. Arizona Press, Tucson, AZ, 1992).

12. Kreslavsky, M. A. & Head, J. W. Kilometre-scale roughness of Mars: Results from MOLA data analysis. *J. Geophys. Res.* **105**, 26695–26711 (2000).
13. Kreslavsky, M. A. & Head, J. W. Mars: Nature and evolution of young latitude-dependent water-ice-rich mantle. *Geophys. Res. Lett.* **29**, doi:10.1029/2002GL015392 (2002).
14. Kreslavsky, M. A. & Head, J. W. Stratigraphy of young deposits in the northern circumpolar region, Mars. *Lunar Planet. Sci.* **XXXIV**, abstr. 1476 (2003).
15. Malin, M. C. & Edgett, K. S. Mars Global Surveyor Mars Orbiter Camera: Interplanetary cruise through primary mission. *J. Geophys. Res.* **106**, 23429–23570 (2001).
16. Mustard, J. F. *et al.* Evidence for recent climate change on Mars from the identification of youthful near-surface ground ice. *Nature* **412**, 411–414 (2001).
17. Seibert, N. M. & Kargel, J. S. Small-scale martian polygonal terrain: Implications for liquid surface water. *Geophys. Res. Lett.* **28**, 899–903 (2001).
18. Mangold, M. *et al.* High latitude patterned grounds on Mars: Evidence for recent melting of near-surface ground ice. *Lunar Planet. Sci.* **XXXIII**, abstr. 1219 (2002).
19. Malin, M. C. & Edgett, K. S. Evidence for recent groundwater seepage and surface runoff on Mars. *Science* **288**, 2330–2335 (2000).
20. Milliken, R. E. *et al.* Viscous flow features on the surface of Mars: Observations from high-resolution MOC images. *J. Geophys. Res.* **108**, doi:10.1029/2002JE002005 (2003).
21. Cabrol, N. A. & Grin, E. A. The recent Mars global warming (MGW) and/or south pole advance (SPA) hypothesis: Global geological evidence and reasons why gullies could still be forming today. *Lunar Planet. Sci.* **XXXIII**, abstr. 1058 (2002).
22. Carr, M. H. Mars Global Surveyor observations of Martian fretted terrain. *J. Geophys. Res.* **106**, 23571–23593 (2001).
23. Kostama, V.-P. *et al.* Morphology of the northern plains in the circumpolar region, Mars. *Lunar Planet. Sci.* **XXXIV**, abstr. 1340 (2003).
24. Costard, F. *et al.* Formation of recent martian debris flows by melting of near-surface ground ice at high obliquity. *Science* **295**, 110–113 (2002).
25. Christensen, P. R. Formation of recent martian gullies through melting of extensive water-rich snow deposits. *Nature* **422**, 45–48 (2003).
26. Hecht, M. H. Metastability of liquid water on Mars. *Icarus* **156**, 373–386 (2002).
27. Boynton, W. V. *et al.* Distribution of hydrogen in the near-surface of Mars: Evidence for subsurface ice deposits. *Science* **296**, 81–85 (2002).
28. Feldman, W. C. *et al.* Global distribution of neutrons from Mars: Results from Mars Odyssey. *Science* **297**, 75–78 (2002).
29. Mitrofanov, I. *et al.* Maps of subsurface hydrogen from the high energy neutron detector, Mars Odyssey. *Science* **297**, 78–81 (2002).
30. Feldman, W. C. *et al.* The global distribution of near-surface hydrogen on Mars. *6th Int. Mars Conf.* Abstr. 5218 (2003).
31. Tokar, R. L. *et al.* Ice concentration and distribution near the south pole of Mars: Synthesis of odyssey and global surveyor analyses. *Geophys. Res. Lett.* **29**, doi:10.1029/2002GL015691 (2002).
32. Mellon, M. T. Theory of ground ice on Mars and implications to the neutron leakage flux. *Lunar Planet. Sci.* **XXXIV**, abstr. 1916 (2003).
33. Jakosky, B. M. & Carr, M. H. Possible precipitation of ice at low latitudes of Mars during periods of high obliquity. *Nature* **315**, 559–561 (1985).
34. Jakosky, B. M., Henderson, B. G. & Mellon, M. T. Chaotic obliquity and the nature of the martian climate. *J. Geophys. Res.* **100**, 1579–1584 (1995).
35. Richardson, M. I. & Wilson, R. J. Investigation of the nature and stability of the Martian seasonal water cycle with a general circulation model. *J. Geophys. Res.* **107**, doi:10.1029/2001JE001536 (2002).
36. Haberle, R. A. *et al.* Orbital change experiments with a Mars general circulation model. *Icarus* **161**, 66–89 (2003).
37. Mischna, M. *et al.* On the orbital forcing of Martian water and CO<sub>2</sub> cycles: A general circulation model study with simplified volatile schemes. *J. Geophys. Res.* **108**, doi:10.1029/2003JE002051 (2003).
38. Richardson, M. I. *et al.* Obliquity, ice sheets, and layered sediments on Mars: What spacecraft observations and climate models are telling us. *Lunar Planet. Sci.* **XXXIV**, abstr. 1281 (2003).
39. Johnson, J. J. & Lorenz, R. D. Thermophysical properties of Alaskan loess: An analog material for the martian polar layered terrain? *Geophys. Res. Lett.* **27**, 2769–2772 (2000).
40. Bockheim, J. G. & Hall, K. J. Permafrost, active-layer dynamics and periglacial environments of continental Antarctica. *S. Afr. J. Sci.* **98**, 82–90 (2002).
41. Marchant, D. R. *et al.* Formation of patterned ground and sublimation till over Miocene glacier ice in Beacon Valley, southern Victoria Land, Antarctica. *Geol. Soc. Am. Bull.* **114**, 718–730 (2002).
42. Williams, P. J. & Smith, M. W. *The Frozen Earth* (Alden, Oxford, UK, 1989).
43. Dixon, J. C. & Abrahams, A. D. *Periglacial Geomorphology* (Binghampton Symp. in Geomorphology: Int. Ser. No. 22, Wiley and Sons, Chichester, 1992).
44. Fanale, F. P. & Salvail, J. R. Quasi-periodic atmosphere-regolith-cap CO<sub>2</sub> redistribution in the Martian past. *Icarus* **111**, 305–316 (1994).
45. Tanaka, K. L. & Scott, D. H. *Geologic map of the Polar Regions of Mars* (Map I-1802-C, Misc. Invest. Ser., US Geological Survey, Reston, VA, 1987).
46. Kolb, E. & Tanaka, K. Geologic history of the polar regions of Mars based on Mars global surveyor data—II. Amazonian period. *Icarus* **154**, 22–39 (2001).
47. Christie-Blick, N. Pre-Pleistocene glaciation on Earth: Implications for climatic history on Mars. *Icarus* **50**, 408–422 (1982).
48. Imbrie, J. Astronomical theory of the Pleistocene ice ages: A brief historical review. *Icarus* **50**, 408–422 (1982).
49. Leovy, C. Weather and climate on Mars. *Nature* **412**, 245–249 (2001).
50. Sugden, D. E. *et al.* Preservation of Miocene glacier ice in East Antarctica. *Nature* **376**, 412–414 (1995).

**Acknowledgements** We acknowledge the many discussions that we had with individuals during the 37th Brown-Vernadsky Microsymposium, held at the Lunar and Planetary Institute on 15–16 March 2003. We also thank J. Dixon, A. Côté and P. Neivert for assistance with manuscript preparation. This work was supported by NASA (J.W.H., J.E.M. and M.A.K.) and the NSF, Polar Programs (D.R.M.).

**Competing interests statement** The authors declare that they have no competing financial interests.

**Correspondence** and requests for materials should be addressed to J.W.H. (James\_Head@brown.edu).